Available online at www.sciencedirect.com
SCIENCE DIRECT®
ELSEVIER
Journal of Molecular Catalysis A: Chemical 207 (2004) 107–116
JOURNAL OF MOLECULAR CATALYSIS A: CHEMICAL
www.elsevier.com/locate/molcata

Estimation of the activation energies for heterogeneous catalytic processes from thermodynamic and structural considerations

S. Harinipriya, M.V. Sangaranarayanan*

Department of Chemistry, Indian Institute of Technology, Chennai 600036, India

Received 3 April 2003; received in revised form 3 July 2003; accepted 4 July 2003

Abstract

The activation energies for three different heterogeneous catalytic processes is evaluated from phenomenogical thermodynamic considerations in conjunction with structural aspects inferred from various mechanistic sequences. The surface coverages of adsorbed species, lattice coordination number of single crystals and polycrystalline metals as well as the corresponding work functions are explicitly incorporated. The reactions considered are the synthesis of ammonia, decomposition of formic acid and hydrogenation of ethylene. The estimated activation energies for the synthesis of ammonia on Fe(1 1 1) and Ru(0 0 0 1) surfaces show satisfactory agreement. In the case of formic acid decomposition, the volcano plot between the activation energy and reaction temperature is rationalized and the subtle role of work functions is indicated. The activation energy for the hydrogenation of ethylene on Pd(1 1 1) and Pt(1 1 1) is estimated and shown to be consistent with the experimental data. A simple phenomenological expression for the activation energy is shown to be valid for three different heterogeneous processes, viz. formation, decomposition and addition reactions.

Keywords: Activation energy; Thermodynamic considerations; Polycrystalline metals

1. Introduction

Over the past several decades, a significant amount of research has been directed towards the design and development of efficient catalysts for a variety of heterogeneous catalytic processes in diverse contexts. However, in view of the specific role played by each catalyst and different reaction pathways constituting a reaction, the estimation of parameters such as activation energy, turn over frequency, etc. has been rendered difficult. Although in situ surface characterization techniques as well as density functional theories pertaining to single crystals, polycrystalline materials and alloys yield valuable insights regarding the role of catalysts, it is preferable to formulate quantitative expressions for estimating kinetic parameters incorporating structural details in conjunction with the experimental data.

In this communication, we provide a phenomenological thermodynamic approach for evaluating the activation energy pertaining to three different heterogeneous catalytic reactions incorporating (i) the nature of the metal via its work function, (ii) influence of adsorbed species using the appropriate surface coverages and (iii) structural considerations deduced from the mechanistic sequence. The illustrative examples chosen in this context are (a) synthesis of ammonia employing single crystals and polycrystalline metals, (b) decomposition of formic acid at various metal surfaces and (c) hydrogenation of ethylene at Pd(1 1 1) and Pt(1 1 1).

The expression for the activation energy should incorporate diverse bonding energies of various adsorbed species and the corresponding surface coverages along with the work function and other structural details of the substrate. At the simplest level of approximation, various energetic contributions may be considered as additive. As the coordination number of the metal (CN_M) increases, the number of active sites available for the catalytic process increases leading to a more facile reaction. Hence the activation energy in general, decreases with increase in CN_M. Thus, the activation energy of any reaction (E_a) is inversely proportional to CN_M. Apart from this, the activation energy depends on the bond formation energies between the metal catalyst and the adsorbing species. The extent of bond formation is determined by the corresponding surface coverages. After adsorption, the adsorbed species might undergo several internal rearrangements to attain a stable configuration

* Corresponding author. Tel.: +91-44-2578269; fax: +91-44-2351365.
E-mail address: mvs@chem.iitm.ac.in (M.V. Sangaranarayanan).

1381-1169/$ – see front matter © 2003 Elsevier B.V. All rights reserved.
doi:10.1016/S1381-1169(03)00500-4

which enables the occurrence of the reaction. This contribution due to the internal rearrangements of the adsorbed species needs to be incorporated in the expression for activation energy. These considerations enable the formulation of E_a as

$$E_a = \left(\frac{1}{CN_M}\right)\{\theta E_{M\text{-ads}} + E_{int\,rearr}\} \quad (1)$$

where $E_{M\text{-ads}}$, θ and $E_{int\,rearr}$ denote the bond formation energy between metal and adsorbate, surface coverage and the energy due to internal rearrangement of the adsobates. The validity of Eq. (1) is demonstrated for the three important heterogeneous catalytic processes mentioned above. It can also be seen that depending on the values of CN_M, $E_{M\text{-ads}}$, θ and $E_{int\,rearr}$ the activation energy of a particular reaction will vary with the catalyst employed.

2. Synthesis of ammonia

On account of its industrial importance, the synthesis of ammonia [1] from N_2 and H_2 using efficient catalysts has been a central focus in heterogeneous catalysis. Among different types of catalysts employed, mention may be made of polycrystalline metals [2], single crystals [3,4], alloys [5] zeolites [6], etc. Several strategies using chemical kinetic schemes [7], adsorption isotherms considerations [8,9], density functional theories [4,10,11] and parallel testing methods for effective screening of catalysts [12] have been formulated so as to obtain new insights into the mechanistic aspects.

2.1. Mechanistic steps and activation energy

The mechanistic steps involved in the synthesis of ammonia using metal catalysts have been postulated as [7]

$$H_2 + M \Leftrightarrow H_{2ads} \quad (2)$$

$$H_{2ads} + M \Leftrightarrow 2H_{ads} \quad (3)$$

$$N_2 + M \Leftrightarrow N_{2ads} \quad (4)$$

$$N_{2ads} + M \rightarrow 2N_{ads} \quad (5)$$

$$N_{ads} + H_{ads} \Leftrightarrow NH_{ads} + M \quad (6)$$

$$NH_{ads} + H_{ads} \Leftrightarrow NH_{2ads} + M \quad (7)$$

$$NH_{2ads} + H_{ads} \Leftrightarrow NH_{3ads} + M \quad (8)$$

$$NH_{3ads} \Leftrightarrow NH_{3(g)} + M \quad (9)$$

where M denotes the surface and the subscript 'ads' indicates the adsorbed entity.

Scheme 1 depicts the visualization of the reaction on the basis of Eqs. (2)–(9). It has been noted that the coordinating sites of the metals play a central role; in the case of Fe(1 1 1), the highly coordinated C_7 sites offer the most favorable situation for adsorption of N_2 and hence facilitates the occurrence of step (4) in the above mechanistic sequence [3].

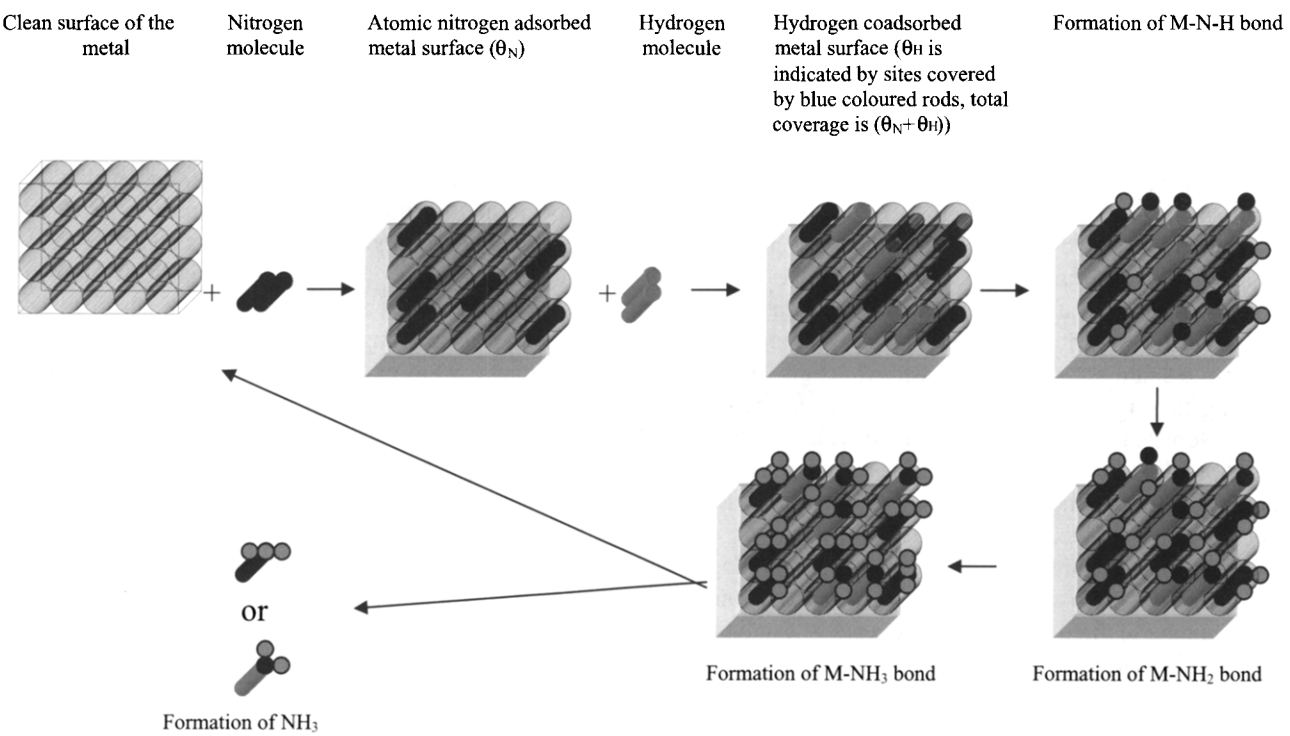

Scheme 1. Schematic representation of the processes involved in ammonia synthesis on metal surfaces (blue rods and circles denote hydrogen atoms, brown rods and circles represent nitrogen atoms, green base denotes metal surface).

Applying Eq. (1) to the above mechanism, we may formulate E_a as

$$E_a = \frac{\theta_H(E_{M-H}+E_{M-NH}+E_{M-NH_2}+E_{M-NH_3}+E_{M,NH_3}) + \theta_N(E_{M-N}+E_{M-NH}+E_{M-NH_2}+E_{M-NH_3}+E_{M,NH_3})}{CN_M} \quad (10)$$

where E_{M-H}, E_{M-N}, E_{M-NH}, E_{M-NH_2}, E_{M-NH_3} represent the formation energy of the appropriate species with the metal M and E_{M,NH_3} is the energy involved in the evolution of ammonia from metal surface. θ_H and θ_N denote respectively the surface coverage of atomic hydrogen and nitrogen.

The salient experimental observations supporting Eq. (10) are as follows: (i) Auger electron spectroscopy (AES) analysis [13] of nitrogen residues on the surface of the Fe catalyst (at high temperatures and pressures) confirms low surface coverage of adsorbed N_2 implying that step (5) may not be the sole rate determining step and this feature is incorporated by including all the surface coverages; (ii) temperature-programmed desorption (TDP) data [14] indicate that both $(N_2)_{ads}$ and N_{ads} are present on the metal surface supporting the "end on" configuration theory and hence the energetics of M–N bond alone may be inadequate for estimating E_a and (iii) among various single crystals of Fe, Fe(1 1 1) in view of its enhanced coordination number is the most effective one, thus validating the inverse proportionality between the activation energy and the coordination number of the metal (CN_M).

2.2. Evaluation of the activation energy

In order to demonstrate the quantitative validity of Eq. (10), various surface coverages appearing in Eq. (10) are required and these have been deduced from the experimental data for Fe(1 1 1) and Ru(0 0 0 1) single crystals (cf. Table 1). The activation energy using the surface coverages ferreted out from recent experimental data and appropriate bond formation energies from tabular compilations yield excellent agreement for Fe(1 1 1)and Ru(0 0 0 1) (cf. Table 1) without employing any adjustable parameters. If promoters (such as alkali metals) [6,20,21] are employed as in the case of Ru-catalyzed ammonia synthesis, their surface coverages along with the coordination number and the appropriate bond formation energetics too need to be incorporated in Eq. (1) which lead to a decrease in E_a vis a vis enhancement in the catalytic activity. For example, if Li is used as the promoter in the case of Fe catalysts, θ_N and θ_H decrease on account of competitive adsorption of Li with N, H and M–Li bond energies too need to be incorporated in Eq. (10). Hence, the promoters decrease the activation energy.

2.3. Influence of the work function of metals

While the incorporation of metallic characteristics using the corresponding lattice coordination numbers is satisfactory, it is more advantageous to have a substrate-dependent parameter which is a direct measure of its electron density. In a variety of applications of density functional theory to metal surfaces and interfaces, the effect of work functions of single crystals and polycrystalline metals has been investigated [8]. Thus, it is of interest to enquire whether the work functions may be directly incorporated into the quantitative expression derived for E_a. A comprehensive analysis to this question requires bond energies and/or surface coverages arising in Eq. (10) in terms of the corresponding work functions. While the exact influence of the work function of a metal on its binding energy with a chosen adsorbate species is un-available, an empirical correlation between metal–hydrogen bonding energies and work functions has been deduced from electrode kinetic data pertaining to nearly 40 metals. Thus, this correlation can be employed to re-write E_{M-H} using the corresponding work functions.

Hydrogen evolution reaction (HER) [22], viz. $H^+ + e \Leftrightarrow (1/2)H_2$ has been studied at different single crystals and polycrystalline metal electrodes using various electrochemical techniques [22,23]. Employing the experimental exchange current densities, E_{M-H} is shown to vary linearly with Φ_M as

$$E_{M-H} = 120 - 11\Phi_M \quad (11)$$

for about 40 metals [22,23] (E_{M-H} is in kcal mol^{-1} and Φ_M is in eV). Thus, Eq. (10) may be re-written as

$$E_a = \frac{\theta_H((120 - 11\Phi_M) + E_{M-NH} + E_{M-NH_2} + E_{M-NH_3} + E_{M,NH_3}) + \theta_N(E_{M-N} + E_{M-NH} + E_{M-NH_2} + E_{M-NH_3} + E_{M,NH_3})}{CN_M} \quad (12)$$

Analogously, it is possible in principle to formulate the bond energies E_{M-N}, E_{M-NH}, E_{M-NH_2}, E_{M-NH_3}, etc. in

Table 1
Estimation of the activation energy for ammonia synthesis using Eq. (10)

Metals	E_{M-H} (eV)	E_{M-N} (eV)	E_{M-NH} (eV)	E_{M-NH_2} (eV)	E_{M-NH_3} (eV)	E_{M,NH_3} (eV)	θ_N	θ_H	CN_M	E_a^{expt} (eV)	E_a^{cald} (eV) from Eq. (10)
Ru(0 0 0 1)	2.98 [4]	5.70 [4]	4.85 [4]	2.95 [4]	0.89 [4]	0.89 [4]	0.25 [4]	0.17 [4]	6 [15]	0.97 [16], 1.05 ± 0.04 [17], 1.10 [4]	0.99
Fe(1 1 1)	0.95 [18,19]	0.48 [18]	0.67 [18]	0.67 [18]	0.67 [18]	0.55 [18]	0.01 [18]	0.012 [18]	7 [3]	0.30 [8]	0.33

The bond energies of all the intermediate species formed on the metal surface are at the reaction temperature. The values of θ_N and θ_H are extracted from the literature [4,8,18].

terms of the metallic work function, thus illustrating the role of the electronic structure of the catalyst in a more rigorous manner. However, no correlations of the type predicted by Eq. (11) exist; nevertheless, the incorporation of Φ_M into the activation energy for heterogeneous catalytic processes seems feasible. Further, since the work functions vary with the nature of single crystals too, their influence on the catalytic activity may also be investigated.

2.4. Nature of catalyst and the activation energy

Ru-based catalysts are extensively employed in the synthesis of ammonia, on account of their less sensitive nature to poisoning. In this context, a recent analysis by Dahl et al. [17] employing diverse Ru-based catalysts deserves mention in so far as the activation energy varies from 69 to 126 kJ mol^{-1}. It is of interest to enquire whether this observation is in accordance with Eq. (10) formulated earlier. In Eq. (10), the nature of the catalyst arises via (i) interaction energies of various adsorbed species with the metal/alloy, (ii) various surface coverages and (iii) the coordination number of the catalyst. Since these parameters play a synergistic role, the activation energies may exhibit a wide variation as observed experimentally [17]. Analogously, the variation of temperature and pressure also influence the surface coverages vis a vis interaction energies even for a chosen catalyst.

3. Decomposition of formic acid

The decomposition of formic acid on metal surfaces has been studied during the past few decades and the synergism between adsorption and catalytic activity has been pointed out [24,25]. Employing different d-metals, it was deduced that metals with lower enthalpy of formation of formates possess higher catalytic activity. The plot between the reaction temperature and the enthalpy of formation of the corresponding metal formates leads to a volcano shaped curve [24] leading to the inference that metals such as Co, Ni, Fe, Cu, Ru, Ir and Pt possess increased catalytic activity while in the case of Pd, Rh, Ag, Au surfaces, the decomposition of formic acid occurs at a lower rate.

Among several single crystals investigated in this context, mention may be made of Fe(1 0 0) [26], W(1 0 0) [27], Ru(1 0 1 0) [28], Cu(1 1 0) [29], Cu(1 0 0) [30], Ni(1 0 0) [31], Ni(1 1 0) [32–34], Ag(1 1 0) [35,36], Pt(1 1 1) [37,38] and Cu/Ni(1 1 0) alloys [39]. Further, different surface characterization and spectroscopic techniques such as high resolution electron energy loss spectroscopy (HREELS), low energy electron diffraction (LEED), AES, multiplexed mass spectroscopy for thermal decomposition spectroscopy (MM-STDS), TPD studies have been employed. It is deduced from these investigations that CO, CO_2 and H_2 may form in general by two different pathways, depending upon the nature of the metal. When single crystal surfaces of Ni and Ru are employed, dehydrogenation occurs by O–H bond cleavage on account of the formation of HCO and HCOO intermediate species [40], which in turn leads to the corresponding metal formates. On the other hand, for single crystals of Fe, W, Cu, Ag, Pt, etc., the cleavage of C–O bond is involved [40]. Hence, the computation of E_a requires invoking two different mechanistic paths as shown in Schemes 2 and 3.

3.1. Mechanistic sequence for formic acid decomposition on Ni and Ru surfaces

The mechanistic sequence for the above reaction may be visualized (Scheme 2) for Ni, Ru, etc. as follows:

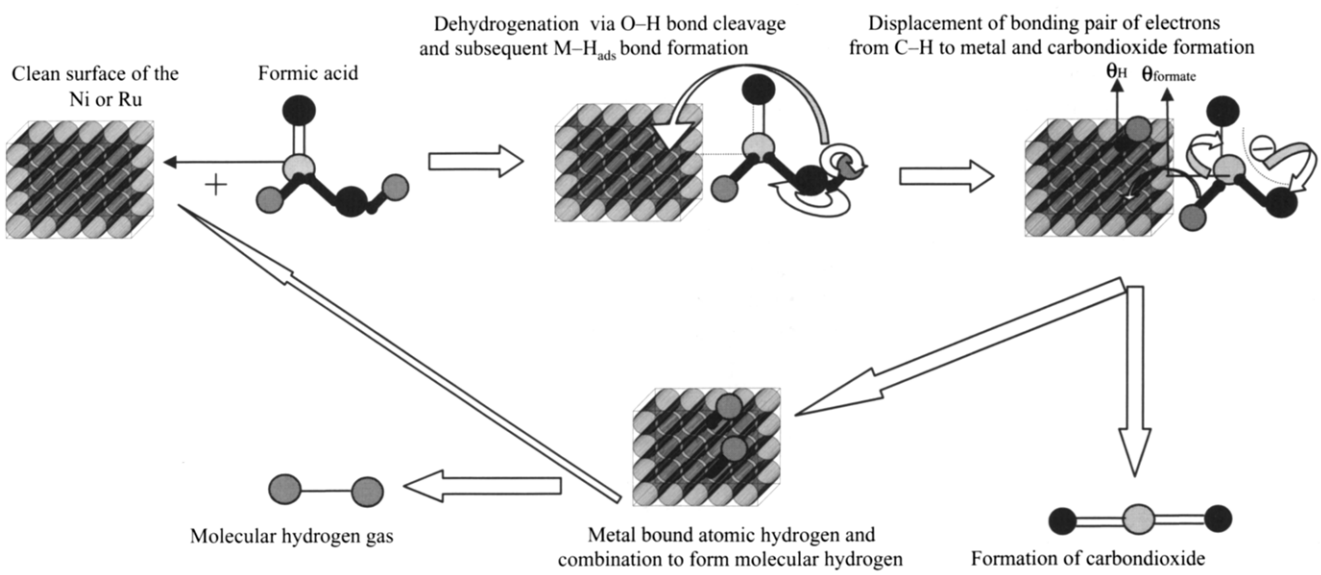

Scheme 2. Representation of steps involved in the decomposition of formic acid on Ni and Ru surfaces (yellow circles denote oxygen atoms, brown rods and lines indicate bonds, blue circles refer to the carbon atoms, red circles represent hydrogen atoms and green base denotes the metal surface). $\theta_{formate}$ is the surface coverage of formic acid and θ_H indicates that of atomic hydrogen.

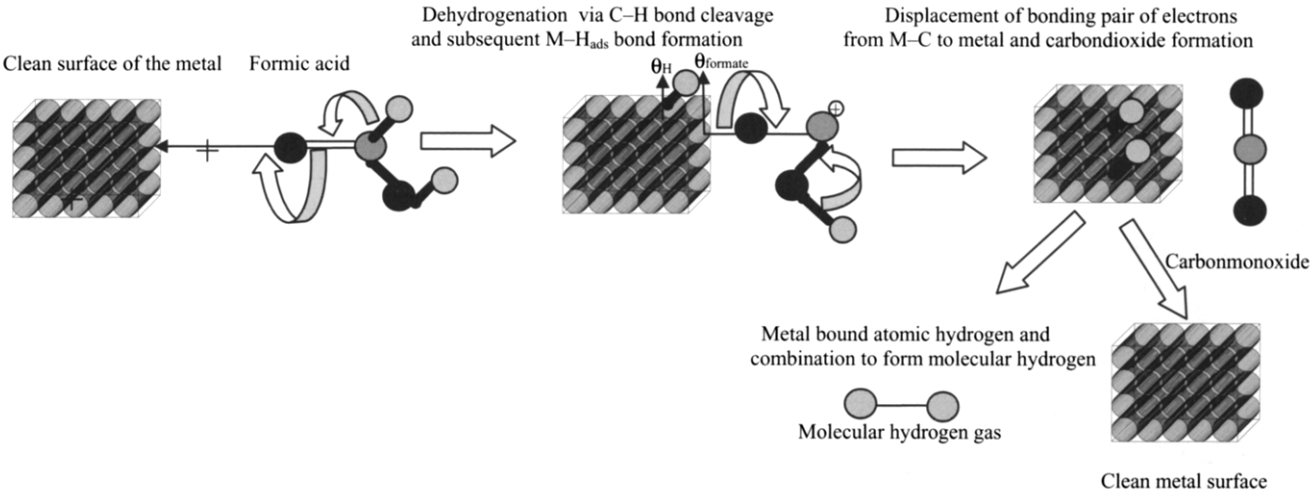

Scheme 3. Representation of steps involved in decomposition of formic acid on metal surfaces such as Cu, Ag, Pt, etc. (yellow circles denote oxygen atoms, brown rods and lines indicate bonds, blue circles refer to the carbon atoms, red circles represent hydrogen atoms and green base denotes the metal surface). $\theta_{formate}$ is the surface coverage of formic acid and θ_H indicates that of atomic hydrogen.

(i) Adsorption of formic acid on the metal leading to the corresponding formate (the energy involved being $E^{form}_{M\text{–formate}}$), viz.

$$M + HCOOH_{(g)} \rightarrow M\text{–}(HCOOH)_{ads} \quad (13)$$

(ii) Dehydrogenation of adsorbed HCOOH via O–H bond cleavage and the energy includes dissociation energy of O–H bond and formation energy of M–H_{ads} (E^{diss}_{O-H}, $E^{form}_{M-H_{ads}}$):

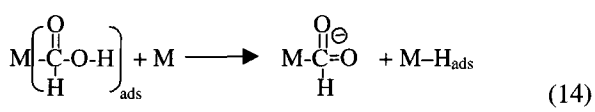

(14)

(iii) Internal rearrangement of the intermediate formed in step (ii) to form $CO_{2(g)}$ via dissociation of M–C, C–H bonds and formation of M–H_{ads} (E^{diss}_{M-C}, E^{diss}_{C-H}, $E^{form}_{M-H_{ads}}$):

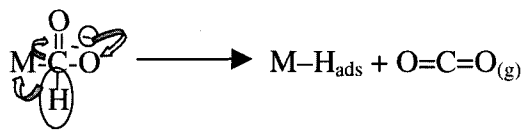

(15)

(iv) Combination of the adsorbed hydrogen atoms to form H_2 gas, $E^{form}_{M-H_{ads}}$ being the energy required for the evolution of $H_{2(g)}$ from the metal surface:

$$2M\text{–}H_{ads} \rightarrow 2M + H_{2(g)} \quad (16)$$

From the above sequence and Scheme 2, the activation energy for decomposition of formic acid on Ni and Ru may be written as

$$E_a = \frac{\theta_{formate}(E^{form}_{M\text{–formate}} + E^{diss}_{M-C}) + \theta_H(2E^{form}_{M-H_{ads}} + E^{form}_{H-H}) + E^{diss}_{O-H} + E^{diss}_{C-H}}{CN_M} \quad (17)$$

where $\theta_{formate}$ represents the surface coverage of formic acid and CN_M denotes the coordination number of the catalyst, as in Eq. (10). The third and fourth terms in Eq. (17) are metal-independent and hence the surface coverages do not occur in these. The surface coverages of adsorbed formates and atomic hydrogen on Ni(1 1 0) are reported to be 0.52 and 0.48, respectively using the Flash decomposition studies [32][1] and in the case of Ni(1 0 0), the coverages $\theta_{formate}$ and θ_H are deduced as 0.59 and 0.41 from LEED investigations [31] (see footnote 1). The values of $E^{form}_{M\text{–formate}}$ and E^{diss}_{M-C} for Ni(1 1 0) and Ni(1 0 0) are estimated as 233.33 and 151.34 kJ mol^{-1} using Morse potentials [41], the coordination number of Ni(1 1 0) and Ni(1 0 0) being 6 [15]. The values of E^{diss}_{C-H}, E^{diss}_{O-H}, E^{form}_{H-H} are available in the tabular compilations as 398.40, 427.60 and −435.99 kJ mol^{-1}, respectively [19]. However, to obtain the activation energy for decomposition of HCOOH on Ni(1 1 0) and Ni(1 0 0) surfaces, the values of $E^{form}_{Ni(1\,1\,0)-H_{ads}}$ and $E^{form}_{Ni(1\,0\,0)-H_{ads}}$ are required and hence Eq. (11) which relates the work function of the metal (Φ_M) to the M–H_{ads} bond dissociation energy is employed. With the help of Eq. (11) and work function of Ni(1 1 0) and Ni(1 0 0) as 5.04 and 5.22 eV, respectively [19], $E^{diss}_{Ni(1\,1\,0)-H_{ads}}$ and $E^{diss}_{Ni(1\,0\,0)-H_{ads}}$ become −270.12 and −261.84 kJ mol^{-1}. These estimates yield the activation energy as 0.96 and 1.14 eV for Ni(1 1 0) and Ni(1 0 0) in satisfactory agreement with the experimental data [31,32] of 1.08 and 1.21 eV.

3.2. Mechanistic sequence for decomposition of formic acid on Cu, Ag, Pt, etc.

The mechanistic sequence for the above reaction may be visualized (Scheme 3) as follows:

[1] The surface coverage of formates and atomic hydrogen are calculated as follows: $\theta = N/N_{sat}$; where N is the coverage of the species on the surface of the metal at a particular temperature, whereas N_{sat} is the coverage of the same at saturation in molecules cm^{-2}.

(i) Adsorption of formic acid on the metal surface ($E^{form}_{M-formate}$):

$$M + HCOOH_{(g)} \rightarrow M\cdots(O{=}CH{-}OH)_{ads} \quad (18)$$

(ii) Dehydrogenation of the metal–formate via C–H bond cleavage, leading to M–H_{ads} (E^{diss}_{C-H}, $E^{form}_{M-H_{ads}}$):

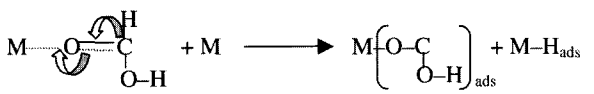

(19)

(iii) Breaking of M–O and O–H bonds with simultaneous M–H_{ads} bond formation occurs yielding CO_2 (E^{diss}_{M-O}, E^{diss}_{O-H}, $E^{form}_{M-H_{ads}}$):

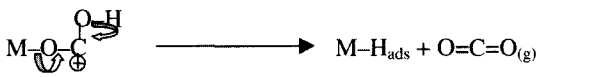

(20)

(iv) Combination of H_{ads} to form $H_{2(g)}$ (E^{form}_{H-H}):

$$2M{-}H_{ads} \rightarrow 2M + H_{2(g)} \quad (21)$$

From the above sequence and Scheme 3, the activation energy for decomposition of formic acid on Ag, Cu, Pt, etc. may be written as

$$E_a = \frac{\theta_{formate}(E^{form}_{M-formate} + E^{diss}_{M-O}) + \theta_H(2E^{form}_{M-H_{ads}} + E^{form}_{H-H}) + E^{diss}_{O-H} + E^{diss}_{C-H}}{CN_M} \quad (22)$$

The surface coverages $\theta_{formate}$ and θ_H on Cu(1 1 0) are reported as 0.61 and 0.39 using AES data [42] (see footnote 1), while the bond energies $E^{form}_{Cu(1\,1\,0)-formate}$, $E^{diss}_{Cu(1\,1\,0)-O}$ are estimated as 315.82 and 79.67 kJ mol^{-1} [41]. The values of E^{diss}_{C-H}, E^{diss}_{O-H}, E^{form}_{H-H} have been tabulated as 398.40, 427.60, −435.99 kJ mol^{-1} [19], while $E^{form}_{Cu(1\,1\,0)-H_{ads}}$ is deduced from Eq. (11) as −295.89 kJ mol^{-1}, employing $\Phi_{Cu(1\,1\,0)}$ as 4.48 eV [19]. Since the coordination number of Cu(1 1 0) is 6 [15], E_a for the decomposition of formic acid on Cu(1 1 0) surface is obtained as 1.15 eV from Eq. (22) in satisfactory agreement with the experimental value of 1.26 eV [42].

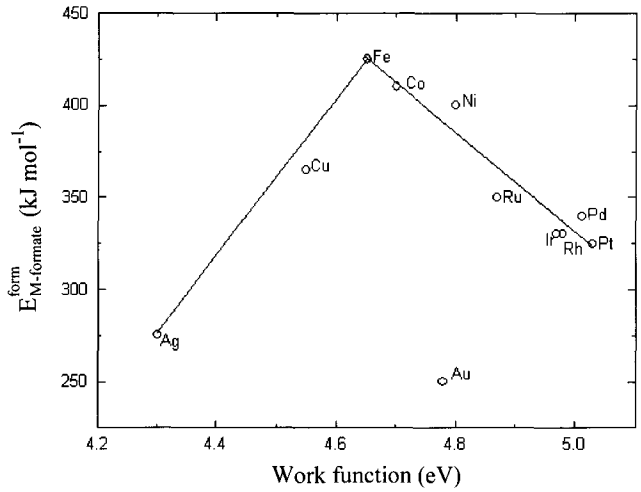

Fig. 1. Relation between the enthalpy of formation of metal formates [24] and work function of the metals [19] for the decomposition of HCOOH on different polycrystalline metal surfaces. Line is drawn as a guide to the eye.

3.3. Influence of work function of metals and stability of metal formates on the activation energy

The foregoing analysis pertains to the evaluation of the activation energy for the decomposition of formic acid on a few selected single crystal surfaces such as Ni(1 1 0), Ni(1 0 0), Cu(1 1 0), etc. However, several investigations involving polycrystalline metals do exist in this context and hence it is imperative to study the validity of Eqs. (17) and (22). Since the surface coverages $\theta_{formate}$ and θ_H pertaining to these polycrystalline metals have not yet been reported, we assume a value of 0.5 for $\theta_{formate}$ and θ_H so as to obtain a few qualitative insights regarding the applicability of Eqs. (17) and (22). Employing these values, the activation energies for the decomposition of formic acid on polycrystalline metal surfaces have been obtained as shown in Table 2.

Table 2
Estimation of the activation energy for HCOOH decomposition from Eqs. (17) and (22) of the text

Metals	$E^{form}_{M-formate}$ (kJ mol^{-1}) [24]	$E^{form}_{M-H_{ads}}$ (kJ mol^{-1}) [19]	E^{diss}_{M-O} (kJ mol^{-1}) [19]	E^{diss}_{M-C} (kJ mol^{-1}) [19]	CN_M [15]	E_a^{cald} from Eq. (17) for Ni and Ru and Eq. (22) for other metals (eV)
Au	−250.00	−292.00	221.80	418.10	6	0.52
Ag	−275.00	−215.10	220.10	385.15	12	0.32
Rh	−330.00	−360.70	391.80	580.00	12	0.24
Pd	−340.00	−268.00	299.20	355.00	12	0.28
Pt	−325.00	−371.50	402.70	598.00	12	0.24
Ir	−330.00	−380.00	414.60	632.00	12	0.23
Ru	−350.00	−234.00	528.40	616.20	12	0.44
Cu	−365.00	−277.80	269.00	393.26	12	0.24
Ni	−400.00	−318.40	382.00	405.35	6	0.50
Co	−410.00	−226.00	384.50	388.50	8	0.48
Fe	−425.00	−180.00	390.40	342.50	12	0.36

The values of $\theta_{formate}$ and θ_H are assumed as 0.5.

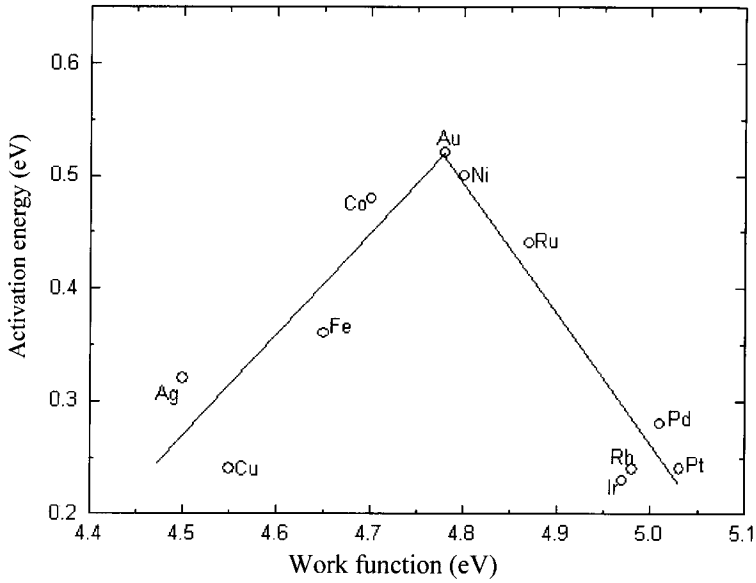

Fig. 2. Correlation between the activation energy calculated from Eqs. (17) and (22) of the text and work function of metals [24].

Table 3
The inter-relationship between the stability of the metal formates, work function of the metals and the activation energy for the decomposition of formic acid

Metals	Metal–formate formation energy, $E^{form}_{M-formate}$	Work function of metals	Activation energy
Left hand side of the volcano plot (Ag, Fe, Cu, Au, etc.)	Increases	Increases from 4.30 to 4.70 eV	Increases
Right hand side of the volcano plot (Co, Ni, Ru, Rh, Ir, Pt, Pd, etc.)	Decreases	Increases from 4.71 to 5.03 eV	Decreases

The stability of the metal formates formed in the first step dictates the overall rate of the decomposition process [24]. Hence, the influence of work function of metals on E_a needs to be investigated. For this purpose, a plot of the enthalpy of formation of metal formates [24] versus work function of metals is constructed, which yields a volcano-shaped plot. On the basis of Fig. 1, we may infer that metals with lower work functions (<4.7 eV) possess enhanced catalytic activity while substrates such as Au, Ni, Ru, Rh, Ir, Pd and Pt having Φ_M values >4.7 eV are less efficient. From the chemical bonding considerations, the electron-releasing tendency of metals and the ability to form bonds with the adsorbates is higher for Ag, Cu, Fe and lower for Co, Ni, Ru, Rh, Ir, Pd and Pt.

The energetic terms $E^{form}_{M-formate}$, $E^{form}_{M-H_{ads}}$ and E^{diss}_{M-C} of Eq. (17) and $E^{form}_{M-formate}$, $E^{form}_{M-H_{ads}}$ and E^{diss}_{M-O} of Eq. (22) are the parameters that vary with the nature of the metal. Thus, a plot of E_a evaluated from Eqs. (17) and (22) versus work function of the metals is constructed and a volcano-shaped dependence is again noticed. From Fig. 2, it follows that the metals which possess moderate work function values (<4.7 eV) act as efficient catalysts for the above reaction with the estimated activation energies ranging from 0.23 to 0.52 eV. These deductions are also supported by the investigation of formic acid decomposition on various d-metals according to which Ag and Au do not possess high catalytic activity in contrast to Fe and Cu.

3.4. Effect of the reaction temperature on the activation energy

Since the activation energy, stability of metal formates and work function of metals are interrelated as indicated in Table 3, an attempt was made to verify the correlation of the reaction temperature with activation energy (Fig. 3) and it was noted that the rate of decomposition of formic acid on Ag and Au is lower in contrast to the metals such as Fe, Cu, etc. This plot provides a rationalization for the volcano plot [43] of $E^{form}_{M-formate}$ versus T.

4. Hydrogenation of ethylene

The hydrogenation of alkenes plays a central role in petroleum cracking and ethylene being the lowest member in the alkene series, it serves as a prototype compound for comprehending the mechanism of hydrogenation. When C_2H_4 is reduced to C_2H_6 on a Pt surface using D_2, $CH_2D–CH_2D$ is formed as the product [44,45], implying that ethylene as well as hydrogen adsorb on Pt with

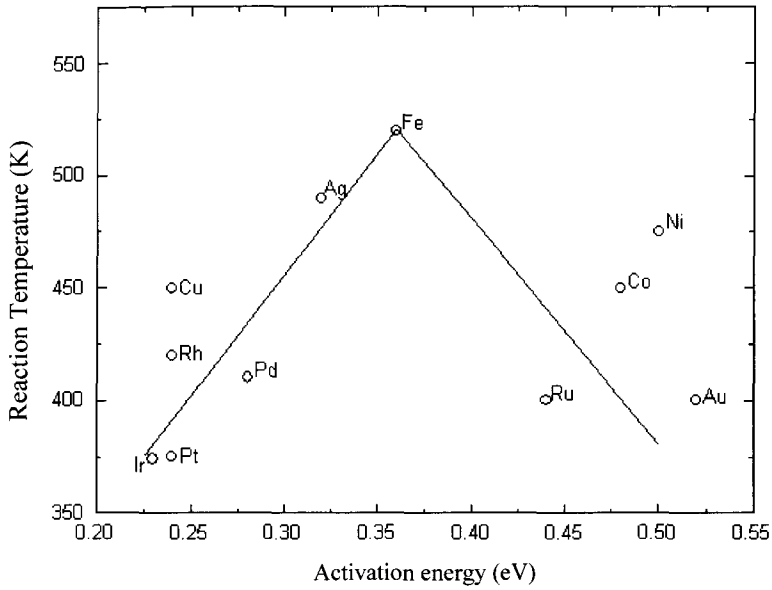

Fig. 3. Reaction temperature [43] vs. activation energy for the decomposition of formic acid on various transition metals as deduced from Eqs. (17) and (22) of the text. Points denote the computed values while the line is drawn as a guide to the eye.

subsequent displacement of adsorbed hydrogen from the metal surface to ethylene. Further, several investigations using ultrahigh vacuum (UHV) and HREELS studies indicate that hydrogenation of ethylene on metal surfaces such as Ni(1 1 0), Pt(1 1 1) and Pd(1 1 1) occurs via the bulk hydrogens existing as metal hydrides [46].

4.1. Mechanistic sequence in the hydrogenation of ethylene on metal surfaces

The mechanism of hydrogenation of ethylene may be represented (Scheme 4) using the following sequential steps:

(1) Adsorption of ethylene forming a metal–π-ethylene complex:

$$CH_2{=}CH_2 + M \Leftrightarrow M{-}CH_2{=}CH_2 \quad (23)$$

(ii) Formation of a metal–di-σ-ethylene complex:

$$M - CH_2 = CH_2 \Leftrightarrow \begin{matrix} CH_2 \text{---} CH_2 \\ \diagdown\ M\ \diagup \end{matrix} \quad (24)$$

(iii) Dissociative adsorption of hydrogen on the metal surface:

$$2M + H_2 \Leftrightarrow 2M{-}H_{ads} \quad (25)$$

(iv) Displacement of adsorbed hydrogen atoms on the metal surface to the metal–di-σ-ethylene complex so as to form metal–ethyl complex:

$$M - H + \begin{matrix} CH_2 \text{---} CH_2 \\ \diagdown\ M\ \diagup \end{matrix} \Leftrightarrow M - CH_2 - CH_3 + M \quad (26)$$

(v) Displacement of neighboring adsorbed hydrogen atoms to the metal–ethyl complex leading to adsorbed ethane, viz.

$$M{-}CH_2{-}CH_3 + M{-}H \Leftrightarrow CH_3{-}CH_{3\,ads} + M \quad (27)$$

(vi) Evolution of ethane gas from the metal surface:

$$(CH_3{-}CH_3)_{ads} \rightarrow (CH_3{-}CH_3)_{(g)} + M \quad (28)$$

In the above sequence, steps (iv) and (vi) provide the support for the isotopic substitution resulting in $DCH_2{-}CH_2D$ as demonstrated from the NEXAFS, TPD and high pressure measurement studies on group IVA metals [45,47,48].

4.2. Estimation of the activation energy

The activation energy, E_a may be represented as

$$E_a = \frac{\theta_{ethylene}(E_{M-\pi\text{-ethylene}} + E_{M\text{-di-}\sigma\text{-ethylene}} + E_{M\text{-ethyl}} + E_{M,ethane}) + \theta_H E^{diss}_{M-H}}{CN_M} \quad (29)$$

where $E_{M-\pi\text{-ethylene}}$, $E_{M\text{-di-}\sigma\text{-ethylene}}$ and $E_{M\text{-ethyl}}$ denote the formation energies of metal–π-ethylene complex, metal–di-σ-ethylene complex and metal–ethyl complex, respectively, while $E^{diss}_{M-H_{ads}}$ and $E_{M,ethane}$ indicate the dissociation energy of metal–hydrogen bond and desorption energy of ethane (gas) from the metal surface, respectively, $\theta_{ethylene}$ and θ_H being the surface coverages of ethylene and hydrogen.

In the case of hydrogenation of ethylene on Pd(1 1 1), the appropriate values of $E_{M-\pi\text{-ethylene}}$, $E_{M\text{-di-}\sigma\text{-ethylene}}$, $E_{M\text{-ethyl}}$, $E_{M,ethane}$ are reported from reflection–absorption infra red spectroscopy (RAIRS) and molecular beam methods [47,49] as 8, 0.1, 13 and $-4.57\,kJ\,mol^{-1}$, respectively, while the coordination number of Pd(1 1 1) is 12. The work function of Pd(1 1 1) is 5.60 eV [19] and hence $E^{diss}_{Pd(1\,1\,1)-H_{ads}}$ is ca. $244.35\,kJ\,mol^{-1}$ from Eq. (12). The surface coverages $\theta_{ethylene}$ and θ_H are estimated from experimental studies as 0.33 and 0.67, respectively [49]. Substituting these values

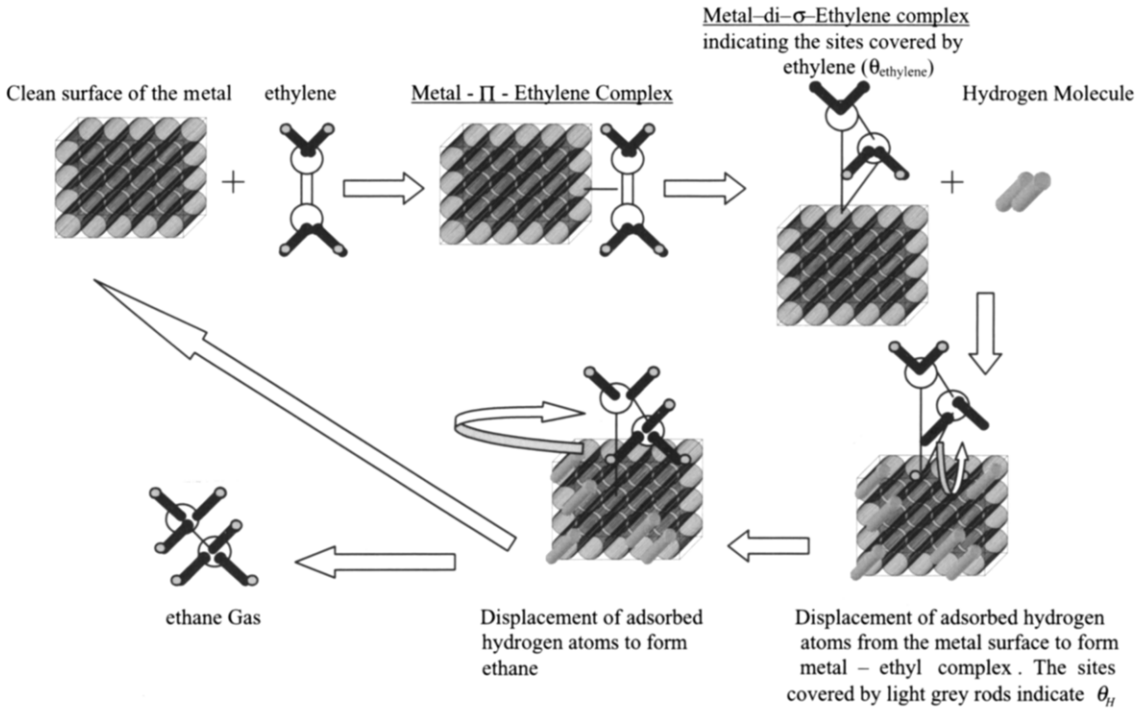

Scheme 4. Representation of steps involved in the hydrogenation of ethylene on metal surfaces (yellow rods and circles indicate hydrogen atoms, brown rods and lines indicate bonds, blue circles denote carbon atoms, green base represents metal surface).

in Eq. (29), the activation energy for the above reaction becomes 0.15 eV which is identical with the experimental data reported using RAIRS and TPD investigations [45].

In a recent study of ethylene hydrogenation on Pt(1 1 1) employing NEXAFS studies [47], the formation energies have been reported for various intermediates (viz. metal–π-ethylene complex as 20.92 kJ mol^{-1}, metal–di-σ-ethylene complex as 0 kJ mol^{-1}, metal–ethyl complex as 25.10 kJ mol^{-1}; whereas the energy involved in the evolution of ethane gas from Pd(1 1 1) surface is reported as −8.37 kJ mol^{-1}).

The surface coverages $\theta_{ethylene}$ and θ_H have not yet been reported for the hydrogenation of ethylene. Hence, $\theta_{ethylene} = \theta_H = 0.5$ is assumed and the metal–hydrogen bond energies are still required. Since the work function of Pt(1 1 1) is 5.63 eV [19] the metal–hydrogen bond dissociation energy from Eq. (12) follows as 242.97 kJ mol^{-1} while the coordination number of Pt(1 1 1) is 6 [15]. Employing these values, the activation energy for ethylene hydrogenation at Pt(1 1 1) is deduced as 0.24 eV in satisfactory agreement with the experimental data of 0.26 eV obtained from UHV studies [50].

5. Perspectives and summary

The foregoing analysis has provided a phenomenological framework whereby the activation energies for heterogeneous catalytic processes may be computed using thermochemical data and structural features. Several important parameters, viz. work functions of the substrate, lattice coordination numbers, relevant surface coverages, energetics of bond formation, etc. appear explicitly in the postulated equations. In order to demonstrate the generality of the formalism, three different classes of reactions, viz. formation, addition and decomposition have been chosen. While all the required parameters pertaining to the synthesis of ammonia have been reported from experimental data thus eliminating the use of adjustable parameters, in the case of the remaining two reactions, the surface coverages being un-available, arbitrary values were employed. Nevertheless, the origin of the volcano plots, the role of metal–formate bond formation energies, etc. are rationalized for the formic acid decomposition thus lending credibility to the assumptions invoked. In the case of ethylene hydrogenation, neither the activation energies nor the trends pertaining to various catalysts are reported thus precluding a direct comparison of our predicted values. Nevertheless, the applicability of macroscopic thermodynamic considerations in conjunction with the visualization of the reaction sequence is a noteworthy feature, apart from the appearance of the work function and lattice coordination number of the catalyst. The latter aspect is especially attractive in so far as it provides a complimentary perspective to the use of local density approximations to heterogeneous catalytic processes thus facilitating suitable design of catalysts.

A few limitations of the methodology need to be pointed out here, viz. (i) the reliability of the parameters employed for various bond energies, (ii) diverse work functions for

several single crystals and polycrystalline metals and (iii) the competitive adsorption between different species and interactions among them. These refinements and their influence on the magnitude of the kinetic parameters requires a detailed analysis.

Acknowledgements

The financial support by the Council of Scientific and Industrial Research, government of India is gratefully acknowledged.

References

[1] K. Tamaru, in: J.R. Jennings (Ed.), Catalytic Ammonia Synthesis: Fundamentals and Practice, Plenum Press, New York, 1991.
[2] A. Mittasch, Adv. Catal. 2 (1950) 81.
[3] N.D. Spencer, R.C. Schoomaker, A.G. Somorjai, J. Catal. 74 (1982) 129.
[4] C.J. Zhang, M. Lynch, P. Hu, Surf. Sci. 496 (2002) 221.
[5] C.J.H. Jacobsen, S. Dahl, S.B. Clausen, S. Bahn, A. Logadottir, K.J. Norskov, J. Am. Chem. Soc. 123 (2001) 8404.
[6] H.-B. Chen, J.-D. Lin, Y. Cai, X.-Y. Wang, J. Yi, J. Wang, G. Wei, Y.-Z. Lin, D.-W. Liao, App. Surf. Sci. 180 (2001) 328.
[7] G. Ertl, in: J. Anderson, M. Boudart (Eds.), Catalysis, Science and Technology, vol. 4, Springer, Berlin, 1983, p. 273.
[8] P. Stoltze, J.K. Norskov, Phys. Rev. Lett. 55 (1985) 2502.
[9] S. Brodsa, C.G. Vayenas, J. Catal. 208 (2002) 38.
[10] (a) A. Logadottir, T.H. Rod, J.K. Norskov, B. Hammer, S. Dahl, C.J.H. Jacobsen, J. Catal. 197 (2001) 229;
(b) S. Dahl, A. Logadottir, C.J.H. Jacobsen, J.K. Norskov, App. Catal. 222 (2001) 19.
[11] T.H. Rod, A. Logadottir, J.K. Norskov, J. Chem. Phys. 112 (2000) 5343.
[12] B. Jandeleit, D.J. Schalfer, T.S. Powers, H.W. Turner, W.H. Weinberg, Angew. Chem. Int. Ed. 38 (1999) 2494.
[13] M.S. Spencer, Catal. Lett. 13 (1992) 45.
[14] H.D. Vandervell, K.C. Vaugh, Chem. Phys. Lett. 171 (1990) 462.
[15] D.M.P. Mingos, Essentials of Inorganic Chemistry, vol. 1, Oxford Science Publications, Oxford University Press, London, 1995, p. 11.
[16] H. Shi, K. Jacobi, G. Ertl, J. Chem. Phys. 102 (1995) 1432.
[17] S. Dahl, E. Taylor, I. Tornquist, I. Chorkendorff, J. Catal. 178 (1998) 679.
[18] M. Bowker, I. Parker, C.K. Waugh, Surf. Sci. 197 (1988) L223.
[19] R.C. Weast (Ed.), CRC Handbook of Chemistry and Physics, 68th ed., CRC Press, Florida, USA, 1987.
[20] D. Szmigiel, H. Bielawa, M. Kurtz, O. Hinrichsen, M. Muhler, W. Rarog, S. Jodzis, Z. Kowalczyk, L. Znak, J. Zielinski, J. Catal. 205 (2002) 205.
[21] R.S. Bare, D.R. Strongin, G.A. Somorjai, J. Phys. Chem. 90 (1986) 4726.
[22] B.E. Conway, Electrochemical Supercapacitors—Scientific Fundamentals and Technological Applications, Kluwer Academic Publishers/Plenum Press, New York, 1999 (Chapter 3).
[23] S. Trasatti, J. Electroanal. Chem. 39 (1972) 163.
[24] M.J.W. Rootsaert, W.M.H. Sachtler, Z. Phys. Chem. 26 (1960) 16.
[25] R. Larsson, H.M. Jamroz, A.M. Borowiak, J. Mol. Catal. 129 (1998) 41.
[26] J.B. Benziger, R.J. Madix, J. Catal. 65 (1980) 49.
[27] J.B. Benziger, E.I. Ko, R.J. Madix, J. Catal. 58 (1979) 149.
[28] L.A. Larson, J.T. Dickinson, Surf. Sci. 84 (1979) 17.
[29] D.H.S. Ying, R.J. Madix, J. Catal. 61 (1980) 48.
[30] B.A. Sexton, Surf. Sci. 88 (1979) 319.
[31] J.B. Benziger, R.J. Madix, Surf. Sci. 79 (1979) 394.
[32] J.G. McCarty, J.L. Falconer, R.J. Madix, J. Catal. 30 (1973) 235.
[33] J.L. Falconer, R.J. Madix, Surf. Sci. 46 (1974) 473.
[34] R.J. Madix, J.L. Falconer, Surf. Sci. 51 (1975) 546.
[35] M.A. Barteau, M. Bowker, R.J. Madix, Surf. Sci. 94 (1980) 303.
[36] B.A. Sexton, R.J. Madix, Surf. Sci. 105 (1981) 177.
[37] N. Abbas, R.J. Madix, Appl. Surf. Sci. 7 (1981) 241.
[38] N. Avery, Appl. Surf. Sci. 14 (1982–1983) 149.
[39] D.H.S. Ying, R.J. Madix, J. Inorg. Chem. 17 (1978) 1103.
[40] R.J. Madix, J.L. Gland, G.E. Mitchell, Surf. Sci. 125 (1983) 481.
[41] E. Shustorovich, A.T. Bell, Surf. Sci. 222 (1989) 371.
[42] I.E. Wachs, R.J. Madix, Surf. Sci. 84 (1979) 375.
[43] D.F. Shriver, P.W. Atkins, C.H. Langford, Inorganic Chemistry, ELBS, Oxford University Press, London, p. 563.
[44] L.P. Wang, W.T. Tysoe, H. Hoffmann, F. Zaera, R.M. Ormerod, R.M. Lambert, Surf. Sci. 94 (1990) 4236.
[45] G.A. Crowder, J. Mol. Spectrosc. 48 (1973) 467.
[46] S.P. Daley, A.L. Utz, T.R. Trautmann, S.T. Ceyer, J. Am. Chem. Soc. 116 (1994) 6001.
[47] D. Stacchiola, S. Azad, L. Burkholder, W.T. Tysoe, J. Phys. Chem. B 105 (2001) 11233.
[48] F. Zaera, G.A. Somorjai, J. Am. Chem. Soc. 106 (1984) 2288.
[49] H. Ofner, F. Zaera, J. Phys. Chem. B 101 (1992) 396.
[50] D. Stacchiola, L. Burkholder, W.T. Tysoe, Surf. Sci. 511 (2002) 215.